DE GRUYTER

Chemical Papers 69 (6) 817–826 (2015)
DOI: 10.1515/chempap-2015-0082

ORIGINAL PAPER

# Performance and characterisation of $CeO_2$–$TiO_2$–$WO_3$ catalysts for selective catalytic reduction of NO with $NH_3$

**Hao Li, Guang-Fei Qu, Yan-Kang Duan, Ping Ning, Qiu-Lin Zhang*, Xin Liu, Zhong-Xian Song**

*Faculty of Environmental Science and Engineering, Kunming University of Science and Technology. Kunming, 650500, China*

Received 19 June 2014; Revised 17 September 2014; Accepted 3 November 2014

Ce-Ti-W-$O_x$ catalysts were prepared and applied to the $NH_3$-selective catalytic reduction (SCR) reaction. The experimental results showed that the Ce-Ti-W-$O_x$ catalyst prepared by the hydrothermal method exhibited higher NO conversion than those synthesised via the sol–gel and impregnating methods, while the optimal content of $WO_3$ and molar ratio of Ce/Ti were 20 mass % and 4 : 6, respectively. Under these conditions, the catalyst exhibited the highest level of catalytic activity (the NO conversion reached values higher than 90 %) across a wide temperature range of 225–450 °C, with a range of gas hourly space velocity (GHSV) of 40000–140000 $h^{-1}$. The catalyst also exhibited good resistance to $H_2O$ and $SO_2$. The influences of morphology, phase structure, and surface properties on the catalytic performance were investigated by $N_2$ adsorption–desorption measurement, XRD, XPS, $H_2$-TPR, and SEM. It was found that the high efficiency of NO removal was due to the large BET surface area, the amorphous surface species, the change to element valence states, and the strong interaction between Ce, Ti, and W.


**Keywords:** selective catalytic reduction, Ce-Ti-W-$O_x$, hydrothermal method, strong interaction

## Introduction

Nitrogen oxides ($NO_x$), largely originating from stationary and automobile sources, are regarded as major atmospheric pollutants which can result not only in acid rain, urban smog, greenhouse effects, and photochemical smog, but also have detrimental effects on human health (Schneider et al., 1994). Many studies have investigated the removal of $NO_x$, and the selective catalytic reduction (SCR) of $NO_x$ with $NH_3$ is a well-proven and widely-used technique (Lee et al., 2013). De-$NO_x$ efficiency by SCR technology is influenced by a number of factors, among which the catalyst plays a significant role. In recent decades, $V_2O_5$–$WO_3/TiO_2$ and $V_2O_5$–$MoO_3/TiO_2$, as the commercial catalysts, have been characterised as exhibiting high activity and extraordinary selectivity between 300 °C and 400 °C (Forzatti, 2001). However, many drawbacks occur in the practical applications, such as a narrow temperature window, poor SCR activity at low temperature, formation of $N_2O$, extra $NH_3$ oxidation at high temperature, and the bio-toxicity of vanadium (Djerad et al., 2006; Liu et al., 2011). Accordingly, the development of vanadium-free $NH_3$-SCR catalysts has attracted extensive attention.

A number of transition metal oxides have been investigated as vanadium-free SCR catalysts (Chmielarz et al., 2014; Ferreira et al., 2010; Li et al., 2013; Liu et al., 2011, 2014; Ma et al., 2013; Qu et al., 2013; Worch et al., 2014). In recent years, cerium-based catalysts, including Ce-Sn-$O_x$ (Li et al., 2013), Ce-Cr-$O_x$ (Liu et al., 2010), Ce-Nb-$O_x$ (Qu et al., 2013), Ce-Al-$O_x$ (Ferreira et al., 2010), $MnO_x$–$CeO_2$ (Wu et al., 2009), $CeO_2$–$MoO_3/TiO_2$ (Liu et al., 2014) have been proposed. The SCR activities over all the above cerium-based catalysts are largely promoted by their impressive oxygen storage capacity, strong mobility of oxygen species, large interactions with metal oxides and

*Corresponding author, e-mail: qiulinzhang_kmust@163.com

the ability of the redox shift between $Ce^{3+}$ and $Ce^{4+}$. $WO_3$, which has been used as an important component of traditional $V_2O_5$–$WO_3/TiO_2$ catalysts, can increase the number of active sites and oxygen vacancies. In addition, the introduction of $WO_3$ enhances the surface acidity of the catalysts which can largely contribute to the absorption of $NH_3$ (Shan et al., 2012). Chen et al. (2011) developed the Ce-W-$O_x$ catalysts via the co-precipitation method, which exhibited excellent SCR activity.

Past research has indicated that $TiO_2$ (which is the favoured support in commercial catalysts for $NH_3$-SCR) can exhibit an excellent sulphur tolerance and promotional effect to catalytic activity (Busca et al., 1998; Gao et al., 2010a). Chen's group (Chen et al., 2010) reported that the Ce-Ti-W-$O_x$ catalysts prepared by the impregnation method assisted with ultrasonic energy exhibited remarkable SCR performance (the $NO_x$ conversion achieved more than 80 %) in the temperature range of 200–450 ℃ under a GHSV of 28000 $h^{-1}$. Shan et al. (2012) found that superior Ce-Ti-W-$O_x$ catalysts produced via a facile homogeneous precipitation method presented excellent activity in $NH_3$-SCR reactions across a wide temperature window of 250–400 ℃.

However, to date few investigations have focused on the preparation of Ce-Ti-W-$O_x$ via the hydrothermal method. Compared with other preparation methods, the hydrothermal method contributes to better dispersion of the active component (Martínez et al., 2012; Pantazis et al., 2005) and catalysts prepared by the hydrothermal method often had larger BET specific surface areas (Li et al., 2005; Zamaro & Miró, 2010).

The results of the current study show that the Ce-Ti-W-$O_x$ catalyst prepared by the hydrothermal method presented greater $NH_3$-SCR activity than those prepared by other methods. The influence of $WO_3$ contents, Ce/Ti molar ratios, GHSV on the activity–structure relationship of Ce-Ti-W-$O_x$ catalyst prepared by the hydrothermal method was further investigated. The resistance to $H_2O$ + $SO_2$ was also studied. XRD, XPS, $N_2$ adsorption–desorption, $H_2$-TPR, and SEM as characterisation methods were introduced to investigate the structures, surface properties, redox abilities and activities of the Ce-Ti-W-$O_x$ catalyst prepared via the hydrothermal method.

## Experimental

### *Catalyst preparation*

All chemicals were supplied by Sinopharm Chemical Reagent Co. (Shanghai, China).

In the hydrothermal method of catalyst preparation, the following solutions were prepared: Solution A: 0.012 mol cerium nitrate, appropriate amount of ammonium paratungstate, 10 mL of deionised water. Solution B: 0.048 mol butyl titanate in 18 mL of acetic acid, 48 mL of absolute ethanol (acetic acid and absolute ethanol were added drop-wise to butyl titanate). Solution C: glucose, acrylic acid, deionised water.

Solutions A, B, and C were mixed in a beaker then ammonia was gradually added to the mixed solution under stirring until pH of 10 was attained, followed by stirring for 5 h. Subsequently, the mixture was poured into the hydrothermal reactor which was placed in the oven at 160 ℃ for 72 h. The mixture thus obtained was filtered then washed several times with deionised water and ethyl alcohol. Then the mixture was first dried at 80 ℃ overnight, the products were calcined at 550 ℃ in $N_2$ for 6 h, and then calcined at 550 ℃ in air for 5 h.

The catalysts with nominal contents of $WO_3$ (5 mass %, 10 mass %, 15 mass %, 20 mass %, 25 mass %, and 30 mass %, denoted as CTW-5%, CTW-10%, CTW-15%, CTW-20%, CTW-25%, and CTW-30%, respectively) were prepared. The influence of molar ratios of Ce/Ti on the SCR performance was further investigated; catalysts with different molar ratios of Ce/Ti (10 : 0, 8 : 2, 6 : 4, 5 : 5, 4 : 6, 2 : 8, and 0 : 10, denoted as CW, C8T2W, C6T4W, C5T5W, C4T6W, C2T8W, and TW, respectively) were achieved with 20 mass % $WO_3$ loading.

The Ce-Ti-W-$O_x$ catalyst with $WO_3$ content of 20 mass % and Ce/Ti ratio of 4 : 6, was prepared using the sol–gel and impregnation methods.

In the sol–gel (SG) method, a mixture of solutions A, B, and C was prepared by the procedure described above, then the mixture was heated at 50 ℃ under vigorous stirring until a transparent yellow sol was obtained. The sol was dried at 70 ℃ for 24 h to form a gel. The product was first calcined at 550 ℃ in $N_2$ for 6 h, then calcined at 550 ℃ in air for 5 h. The catalyst obtained via the sol–gel method was denoted as CTW-SG.

In the impregnating (IM) method, an aqueous solution containing cerium nitrate and ammonium paratungstate was prepared then the commercial $TiO_2$ was immersed in the solution for 6 h. The sample was heated to 60 ℃ for 2 h and 70 ℃ for 3 h. Next, the powder was dried at 105 ℃ overnight, followed by calcination at 550 ℃ in air for 5 h. The catalyst prepared via the impregnating method was denoted as CTW-IM.

### *Catalyst activity test and characterisation*

The activity test was conducted in the vertical fixed-bed reactor (i.d. = 10 mm) using 1 mL of catalysts of 60–80 mesh particle size. The simulated gas, which was controlled by a mass-flow controller, contained 0.06 vol. % of $NH_3$, 0.06 vol. % of NO, 5 vol. % of $O_2$, and $N_2$ for balance. The total flow-rate was 400 mL $min^{-1}$ under the GHSV of 60000 $h^{-1}$. The experimental equipment required for analysing

the tail gas was a Flue Gas Analyser (ECOM · J2KN, rbr Messtechnik, Iserlohn, Germany). The catalytic performance was tested at each temperature after the reaction system had reached a steady state.

The correlations between the catalytic activities and structures were illustrated via different characterisation techniques. Powder XRD patterns of catalysts were obtained on a Bruker D8 Advance X-ray diffractometer (Burke Corporation, Germany) with the angle of $2\theta$ between 10° and 70° operating at 40 kV and 40 mA using Cu$K_\alpha$ radiation. The nitrogen adsorption–desorption isotherms were acquired at liquid $N_2$ temperature (–196 ℃) using a Tristar II 3020 adsorption instrument (Micromeritics Instruments, USA). Prior to the measurement, the samples were evacuated at 100 ℃ for at least 6 h under vacuum conditions. The specific surface areas were evaluated using the Brunauer–Emmett–Teller (BET) equation. Pore size distributions and average pore diameters were confirmed using the Barrett–Joyner–Halenda (BJH) method. The X-ray photoelectron spectrum (XPS) was observed on an ULVAC PHI 5000 VersaProbe II equipment (ULVAC PHI, Japan). The spectra observed were corrected by the C 1s binding energy value of 284.6 eV. $H_2$-temperature-programmed reduction ($H_2$-TPR) experiments were carried out in a home-made quartz reactor under $H_2$/Ar flow (30 mL min$^{-1}$) at a heating rate of 10 ℃ min$^{-1}$ up to 850 ℃. The products were analyzed using gas chromatograph equipment (Fuli-9790, Fujian, China). Prior to the $H_2$-TPR experiments, 100 mg of each sample was pretreated at 450 ℃ in $N_2$ (30 mL min$^{-1}$) for 45 min then cooled to 100 ℃. The scanning electron micrographs (SEM) of samples were recorded using a Hitachi field emission scanning electron micrograph (Hitachi, Japan).

## Results and discussions

### *Activity test*

Fig. 1 shows that the nominal $WO_3$ content has a visible influence on $NO_x$ conversion. It is noted that the NO conversion of all these catalysts can attain almost 100 % within the temperature window range from 200 ℃ to 400 ℃. At low temperatures (175 ℃ or below), with the increase in the $WO_3$ loading, the NO conversion was enhanced until the $WO_3$ content in the catalyst attained 20 mass %. With the $WO_3$ content further increasing, the NO conversion apparently decreased. As the $WO_3$ content increased from 5 mass % to 20 mass %, the temperature window was extended but reduced at higher $WO_3$ loading. Fig. 1 shows that the NO conversion of CTW-5% and CTW-15% decreased sharply when the temperature reached 425 ℃, which distinguished it from the other samples. Furthermore, the NO conversion over CTW-20% was higher than CTW-25% and CTW-30%

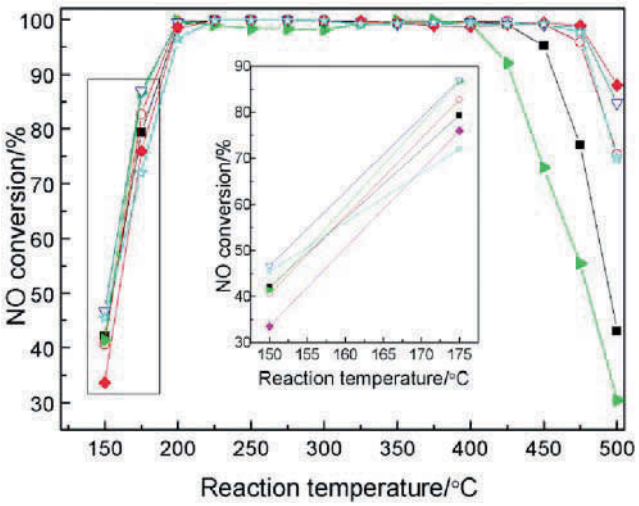


**Fig. 1.** NO conversion on Ce-Ti-W-$O_x$ catalysts (molar ratio: Ce : Ti = 2 : 8) with various $WO_3$ content: CTW-5% (■), CTW-10% (○), CTW-15% (▶), CTW-20% (▽), CTW-25% (♦), and CTW-30% (☆). Reaction conditions: [NO] = [$NH_3$] = 0.06 vol. %, [$O_2$] = 5 vol. %, $N_2$ for balance, GHSV = 60000 h$^{-1}$.

at low temperatures. In summary, the optimal $WO_3$ loading was 20 mass % and the NO conversion of CTW-20% could achieve more than 90 % across a wide temperature range of 180–490 ℃ with the GHSV of 60000 h$^{-1}$ employed.

After the optimal content of $WO_3$ was selected, a series of Ce-Ti-W-$O_x$ catalysts with various molar ratios of Ce/Ti were prepared and tested. Fig. 2 shows that the molar ratios of Ce/Ti and the NO conversion are not linearly related. It is evident that the Ti-W-$O_x$ catalysts exhibited limited SCR activity below 400 ℃. Nevertheless, the activities of the Ce-Ti-W-$O_x$ catalysts at low temperature were greatly enhanced by the introduction of Ce. Among these Ce-Ti-W-$O_x$ catalysts, with the decreasing Ce/Ti ratio, the NO conversion increased markedly at temperatures above 425 ℃. At low temperatures (below 200 ℃), the NO conversion clearly increased while the Ce/Ti ratio decreased from 8 : 2 to 4 : 6. However, when the Ce/Ti ratio decreased to 2 : 8, the catalyst exhibited poor low-temperature activity.

As illustrated in Fig. 2, the CW catalyst also possessed excellent SCR activity. Compared with the bi-component catalyst, the C4T6W catalyst showed improved catalytic performance at both ends of the interval. Hence, it was discovered that the most active catalyst was obtained with the Ce/Ti ratio of 4 : 6.

Since working under high space velocity is very important to practical use of the $NH_3$-SCR catalyst, the influence of the GHSV on NO conversion was investigated by varying the GHSV over the C4T6W catalyst. As shown in Fig. 3, the NO conversion over C4T6W apparently decreased with the increase in the space velocity from 40000 h$^{-1}$ to 140000 h$^{-1}$ at low temperatures. However, there is no detectable influence

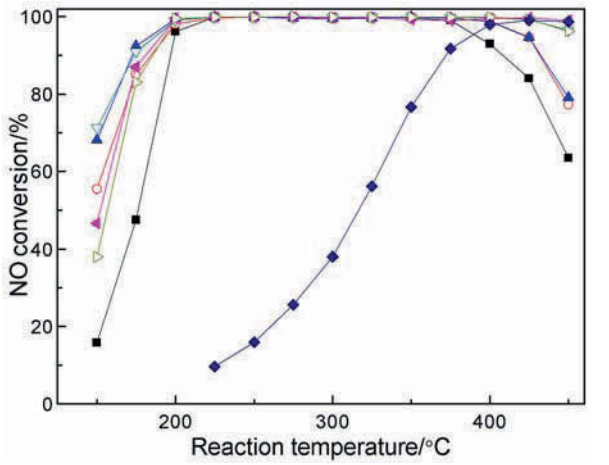


**Fig. 2.** NO conversion on Ce-Ti-W-$O_x$ catalysts with various molar ratios of Ce/Ti: C8T2W (■), C6T4W (○), C5T5W (▲), C4T6W (▽), C2T8W (◀), CW (▷), TW (◆). Reaction conditions: [NO] = [$NH_3$] = 0.06 vol. %, [$O_2$] = 5 vol. %, $N_2$ for balance, GHSV = 60000 $h^{-1}$.

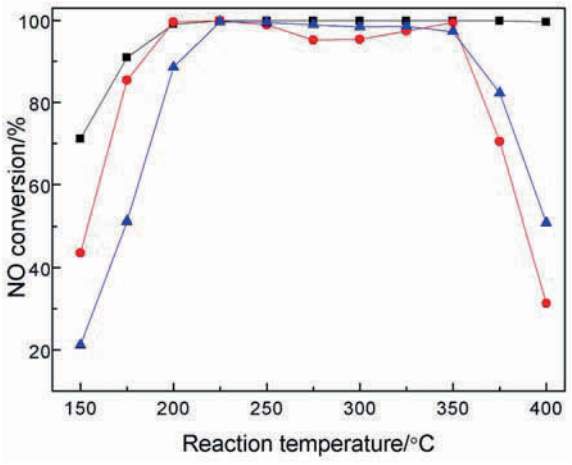


**Fig. 4.** NO conversion of Ce-Ti-W-$O_x$ catalysts prepared by different methods: C4T6W (■), CTW-SG (●), CTW-IM (▲). Reaction conditions: [NO] = [$NH_3$] = 0.06 vol. %, [$O_2$] = 5 vol. %, $N_2$ for balance, GHSV = 60000 $h^{-1}$.

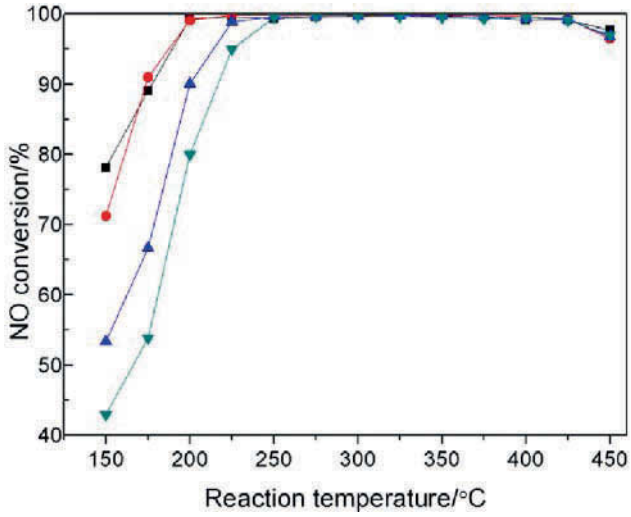


**Fig. 3.** NO conversion of Ce-Ti-W-$O_x$ catalysts at various GHSV/$h^{-1}$: 40000 (■), 60000 (●), 100000 (▲), 140000 (▼). Reaction conditions: [NO] = [$NH_3$] = 0.06 vol. %, [$O_2$] = 5 vol. %, $N_2$ for balance.

on the catalytic activity above 250 ℃ under various GHSVs. Even with the GHSV as high as 140000 $h^{-1}$, the C4T6W catalyst was effective in NO reduction in the range of 225–450 ℃. As, under normal conditions, the diesel engine often operates under a wide range of temperature and flow, the catalysts for the removal of $NO_x$ from the diesel exhaust are required to possess high and stable NO conversion under variable GHSVs. The experimental results showed that the catalytic performance of the C4T6W catalyst exhibited a fairly high level throughout a broad temperature scope under a wide range of GHSV from 40000 $h^{-1}$ to 140000 $h^{-1}$ employed. The effect of GHSV on NO conversion over C4T6W was insignificant, which met the dynamic operating conditions of the diesel engine exhaust. Hence, the C4T6W was regarded as a promising candidate for NO abatement from the diesel exhaust.

The $NH_3$-SCR activities over catalysts prepared via different methods are shown in Fig. 4. It was clear that C4T6W prepared using the hydrothermal method exhibited the highest catalytic activity and afforded the widest temperature window. The SCR activity of CTW-SG was higher than that of CTW-IM at temperatures below 225 ℃. Nevertheless, the catalytic activity of CTW-SG was lower than that of CTW-IM at high temperatures. Hence, the Ce-Ti-W-$O_x$ catalyst prepared by the hydrothermal method exhibited higher NO conversion than those prepared via the sol–gel and impregnation methods.

As $H_2O$ and $SO_2$ are the main components in the diesel exhaust and often lead to deactivation of the catalysts, the resistance of C4T6W to $SO_2$ and $H_2O$ + $SO_2$ in the SCR system was also investigated. Fig. 5 shows that, when 0.01 vol. % $SO_2$ was added to the simulated gas, a sharp decrease in the NO conversion could be observed below 250 ℃. The inhibiting effect was greater with the co-presence of $H_2O$ + $SO_2$ at low temperatures. The decline in NO conversion in the presence of $SO_2$ or $H_2O$ + $SO_2$ might be explained as the deposition of ammonium bisulphate and the effect of a competitive adsorption between $H_2O$ and $NH_3/NO_x$ (Yang et al., 2011; Amiridis et al., 1996). However, the catalytic performance of C4T6W was enhanced at temperatures above 450 ℃ in the presence of $SO_2$ or $H_2O$ + $SO_2$, which could be ascribed to the increase in the surface acidity of the catalyst (Long & Yang, 1999).

For further study, the deactivation of C4T6W at 300 ℃ was investigated. The inset in Fig. 5 shows that the SCR reaction stabilised for 60 min at 300 ℃ with-

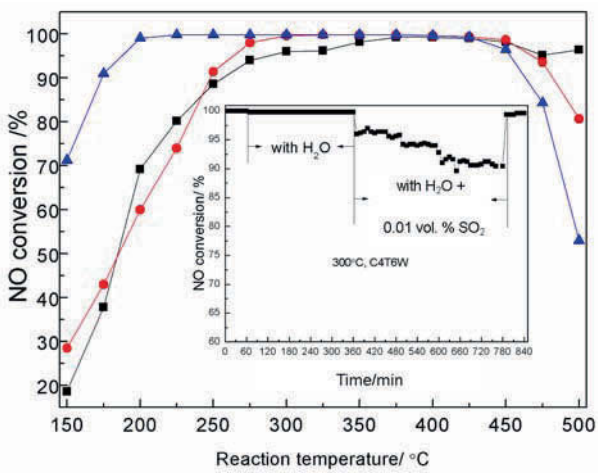


**Fig. 5.** NO conversion over C4T6W catalyst in the absence (▲) and presence of $SO_2$ (●) and $H_2O + SO_2$ (■). Reaction conditions: [NO] = [$NH_3$] = 0.06 vol. %, [$O_2$] = 5 vol. %, [$H_2O$] = 10 vol. %, [$SO_2$] = 0.01 vol. %, $N_2$ for balance, GHSV = 60000 $h^{-1}$.

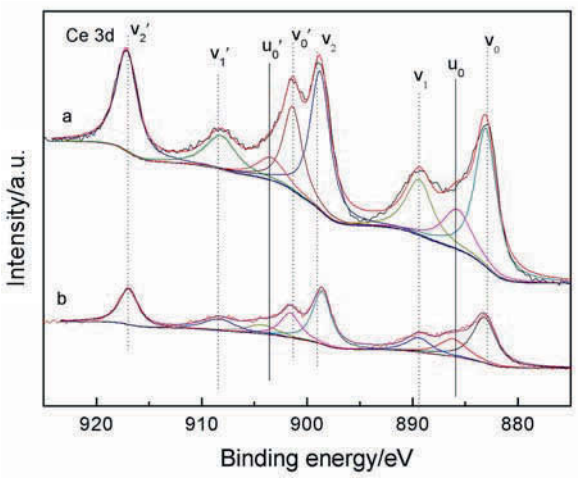


**Fig. 7.** XPS spectra of Ce 3d of CW (a) and C4T6W (b) catalysts.

out $H_2O$ and $SO_2$. After 10 vol. % of $H_2O$ was added to the reactants, the NO conversion retained its original level for 5 h, revealing that C4T6W had excellent resistance to $H_2O$. When 10 vol. % of $H_2O$ and 0.01 vol. % of $SO_2$ were added to the reaction gas mixture, the NO conversion over C4T6W held steady with only a slight decrease to 90 % over a period of almost 7 h. When $H_2O$ and $SO_2$ were removed, the catalytic performance of C4T6W recovered rapidly. The results indicated that the inhibiting effect of $H_2O$ and $SO_2$ was reversible. Hence, C4T6W exhibited good resistance to $H_2O$ and $SO_2$ at 300 °C.

### *Results of catalyst characterisation*

Fig. 6 shows the XRD patterns of Ce-Ti-W-$O_x$ catalysts with various Ce/Ti molar ratios and different $WO_3$ contents. The XRD patterns of commercial $TiO_2$ (supplied by Hangzhou Wanjing New Material Co., China) were also introduced as a reference. Fig. 6 shows that no visible diffraction peaks of $CeO_2$ were observed for C4T6W and C2T8W. It may be concluded that the phase structure of C4T6W and C2T8W catalysts is amorphous.

While the molar ratio of Ce/Ti achieved 5 : 5, cubic $CeO_2$ oxide (PDF-ICDD 34-394) was detected. Similar diffraction peaks were found in cerium-rich samples. Otherwise, the structure of Ce-Ti-W-$O_x$ catalysts with different contents of $WO_3$ (the molar ratio of Ce/Ti = 2 : 8) was also amorphous. This confirmed the conclusion above that the $TiO_2$-rich samples tended to be amorphous in structure. It was notable that no obvious crystalline phase ascribed to $WO_3$ appeared in all the samples, indicating a bet-

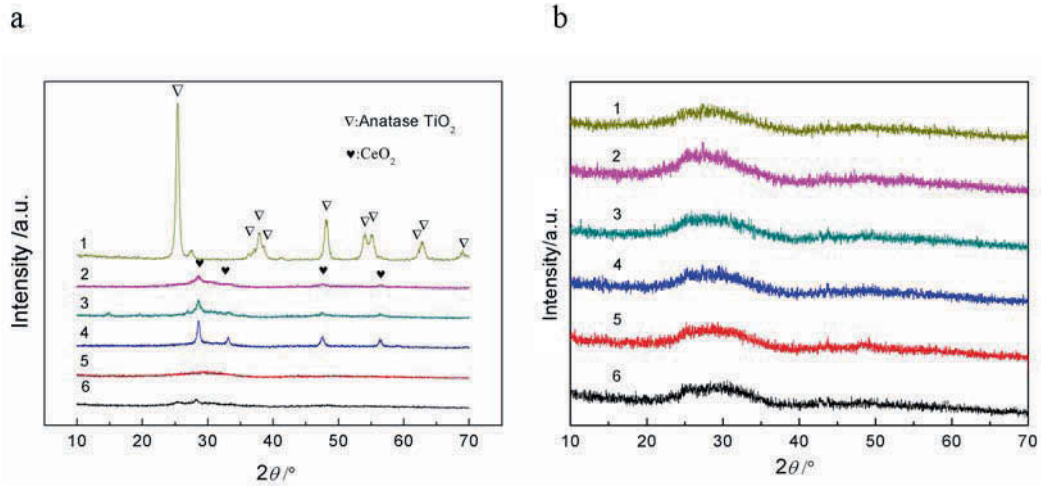


**Fig. 6.** XRD patterns of Ce-Ti-W-$O_x$ catalysts with various molar ratio of Ce/Ti (a): pure $TiO_2$ (1), C8T2W (2), C6T4W (3), C5T5W (4), C4T6W (5), C2T8W (6) and various W content (b): CTW-30% (1), CTW-25% (2), CTW-20% (3), CTW-15% (4), CTW-10% (5), CTW-5% (6).

**Table 1.** Results from $N_2$ adsorption–desorption experiments using different catalysts

| Samples | BET surface area | Total pore volume | Average pore diameter |
|---|---|---|---|
| | $m^2\ g^{-1}$ | $mL\ g^{-1}$ | nm |
| CTW-5% | 213 | 0.267 | 28 |
| CTW-10% | 236 | 0.296 | 25 |
| CTW-15% | 186 | 0.222 | 32 |
| CTW-20% | 192 | 0.265 | 31 |
| CTW-25% | 173 | 0.193 | 35 |
| CTW-30% | 149 | 0.142 | 40 |
| C4T6W | 128 | 0.100 | 47 |
| C5T5W | 106 | 0.112 | 49 |
| C6T4W | 64 | 0.041 | 95 |
| C8T2W | 21 | 0.017 | 285 |
| CW | 43 | 0.087 | 141 |
| TW | 148.9 | 0.163 | 45 |

**Table 2.** Atomic composition of C4T6W, TW, and CW catalysts using XPS

| Catalyst | Surface atomic concentration/at. % | | | | | |
|---|---|---|---|---|---|---|
| | Ce | Ti | W | O | $Ce^{3+}/(Ce^{4+} + Ce^{3+})$ | $O_\alpha/(O_\alpha + O_\beta + O_\gamma)$ |
| C4T6W | 12.72 | 15.04 | 4.08 | 68.17 | 20.1 | 51.1 |
| TW | – | 21.89 | 4.45 | 73.57 | – | 32.5 |
| CW | 30.35 | – | 2.44 | 67.21 | 19.4 | 39.4 |

ter distribution of $WO_3$ or formation of solution. Due to the acidic properties due to $WO_3$, the better distribution of $WO_3$ also means that more acid sites can be offered. From the results of the SCR activity, it could be seen that the formation of cubic $CeO_2$ oxide might inhibit the catalytic performance, especially at higher temperatures.

The BET specific surface areas, total pore volumes, and average pore diameters of all the samples are presented in Table 1. According to Table 1, with the increase in the $WO_3$ content, no obvious rule for variation of the BET surface area could be identified. All of the $TiO_2$-rich samples had a large BET surface area and a small average pore diameter. In addition, it was known that a large BET surface area could provide abundant surface active sites and lead to better dispersion of the active components. Nevertheless, the CTW-10% catalyst with the largest BET surface areas (236.3 $m^2\ g^{-1}$) did not exhibit the best SCR activity, suggesting that the specific surface areas had exceeded the threshold value. Moreover, in the case of the catalysts with different molar ratios of Ce/Ti, it was notable that the decrease in Ti resulted in a sharp decrease in the BET surface areas from 193.3 $m^2\ g^{-1}$ to 21.1 $m^2\ g^{-1}$, i.e. the specific surface area was proportional to the amount of Ti, which was in accordance with the XRD results; the agglomeration of the surface species was caused by $CeO_2$ crystallites, leading to the decrease in surface area. As a consequence, the BET surface area of these $TiO_2$-rich samples was not a key factor in the SCR reaction.

In order to elucidate the information on the chemical state and atomic concentration of various elements, the samples were investigated by XPS spectroscopy. The surface elemental composition of various catalysts is presented in Table 2, and the narrow spectra are listed and discussed seriatim in the following text.

The photoelectron spectra of Ce 3d are displayed in Fig. 7. The two binding energy peaks centred at 886 eV and 904 eV, which were denoted as $u_0$ and $u_0'$, were assigned to $Ce^{3+}$ while the others to $Ce^{4+}$ species (Gupta et al., 2009). The surface relative molar ratios of $Ce^{3+}/(Ce^{3+} + Ce^{4+})$ in CW and C4T6W are summarised in Table 2. An increase in the ratio of $Ce^{3+}/(Ce^{3+} + Ce^{4+})$ could be seen for C4T6W (20.1 %) compared with CW (19.4 %), as shown in Table 2. It could be concluded from this that the amount of $Ce^{3+}$ increased slightly with the introduction of Ti. As reported in the literature (Liu et al., 2013; Li et al., 2011), charge imbalance, oxygen vacancies, and unsaturated bonds were created due to the presence of $Ce^{3+}$, which was crucial for the increase of chemisorbed oxygen amount. Furthermore, $Ce^{3+}$ sites also had positive effects on the redox abilities due to the oxidation of $Ce^{3+}$ to $Ce^{4+}$. This conclusion corresponds to the excellent catalytic activity of C4T6W, especially within the low-temperature range.

The photoelectron peaks of O 1s (Fig. 8) could be fitted into three binding energy peaks, corresponding to lattice oxygen (529.3–530.0 eV, denoted as $O_\beta$), chemisorbed oxygen (531.3–531.9 eV, denoted as $O_\alpha$), and surface hydroxyls (532.7–533.5 eV, denoted as $O_\gamma$,

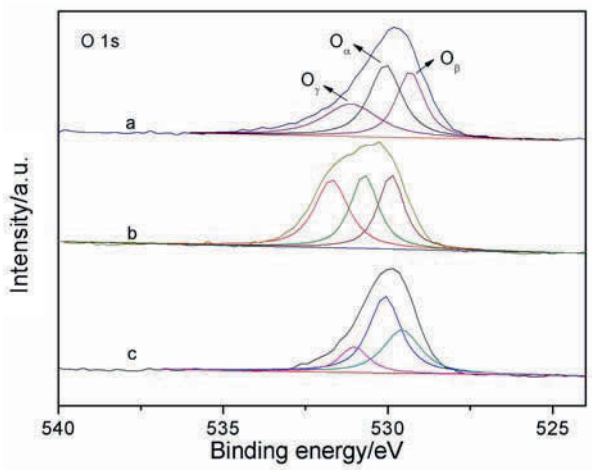


**Fig. 8.** XPS spectra of O 1s of CW (a), TW (b), and C4T6W (c) catalysts.

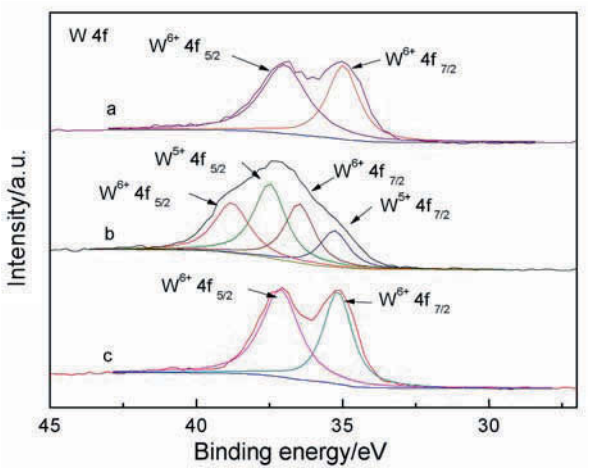


**Fig. 9.** XPS spectra of W 4f of CW (a), TW (b), and C4T6W (c) catalysts.

Peng et al. (2013)). In the case of the cerium-based samples, an obvious shift towards lower binding energy values can be observed in comparison with the TW catalyst. This also implies that a strong interaction existed between O and the other surface species. The concentration ratios of $O_\alpha/(O_\alpha + O_\beta + O_\gamma)$ for the samples were also calculated and shown in Table 2. Table 2 shows that the ratios of $O_\alpha/(O_\alpha + O_\beta + O_\gamma)$ for C4T6W (51.1 %) were higher than those for CW (39.4 %), which represented a similar trend to that shown by $Ce^{3+}/(Ce^{3+} + Ce^{4+})$. This result indicated that the higher amount of $Ce^{3+}$ had a positive effect on the formation of $O_\alpha$. It has been reported that, on account of its higher mobility than that of lattice oxygen ($O_\beta$) and facilitation of the NO oxidation to $NO_2$ (the "fast SCR" reaction is promoted while the ratio of $NO/NO_2$ is close to 1 : 1, e.g. Ruggeri et al. (2012)), surface chemisorbed oxygen ($O_\alpha$) was often regarded as the most active oxygen species, which was beneficial for the improvement of catalytic performance (Jing et al., 2001). It should be noted that the ratios of $O_\alpha/(O_\alpha + O_\beta + O_\gamma)$ for the cerium-containing samples were higher than that for the TW catalyst, demonstrating that the Ce plays a dominant role in the improvement of SCR activity at low temperature.

The XPS spectra of W 4f of various catalysts are shown in Fig. 9. The binding energies of the W 4f peaks for the TW catalyst were assigned to W $4f_{7/2}$ and W $4f_{5/2}$, respectively. As shown in Fig. 9, the binding energy peaks for W 4f of TW were further separated into four peaks. The binding energy peaks at approximately 35.2 eV and 37.5 eV were assigned as $W^{5+}$ species, while the binding energy peaks at 36.5 eV and 38.7 eV corresponded to $W^{6+}$ (Zhang et al., 2012). With the addition of Ce, similar binding energy peaks of W 4f of the cerium-containing samples could be obtained. Their close symmetry led to the two binding energy peaks of C4T6W and CW being

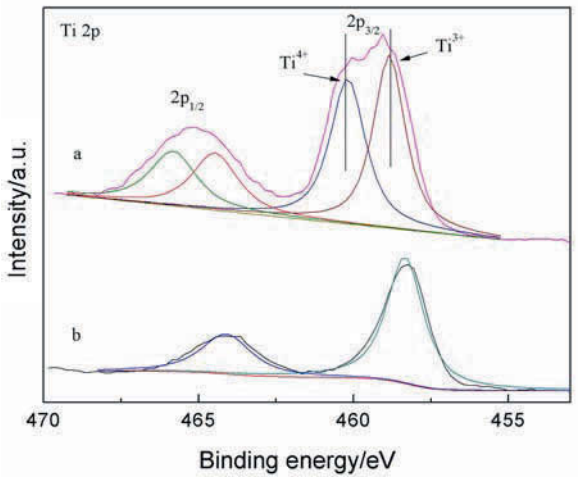


**Fig. 10.** XPS spectra of Ti 2p of TW (a) and C4T6W (b) catalysts.

attributed to $W^{6+}$ species (Chen et al., 2011). Compared with TW, there was a noticeable shift toward low binding energy values over the cerium-containing samples. These phenomena could be explained by the deficiency of Ce with intense electronegativity, suggesting the intense interaction between Ce and W.

Fig. 10 shows the binding energies of the Ti 2p photoelectron peaks for the TW and C4T6W catalysts, corresponding to Ti $2p_{3/2}$ and Ti $2p_{1/2}$ lines, respectively. The overlapping Ti 2p peaks were separated into a number of peaks, and the XPS peaks for Ti $2p_{3/2}$ of the TW catalyst were further divided into two peaks. The binding energy peak centred at 460 eV was assigned to $Ti^{4+}$ species. The binding energy values for $Ti^{3+}$ were reported to be lower than those for $Ti^{4+}$ (Qu et al., 2013; Reddy Inturi et al., 2014), hence the binding energy peak centred at 459 eV was ascribed to $Ti^{3+}$. When doped with Ce, the Ti 2p

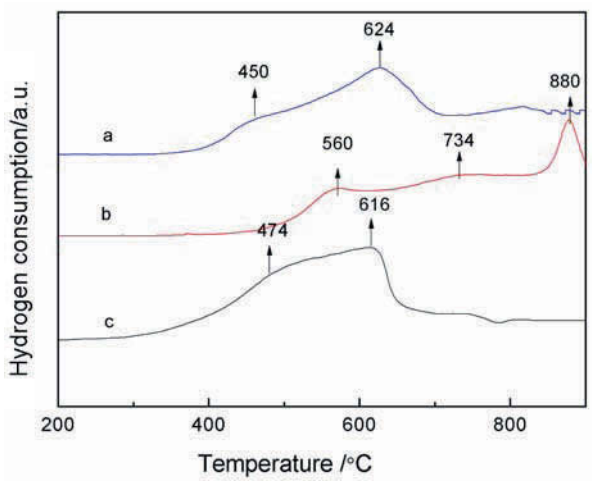


**Fig. 11.** $H_2$-TPR profiles of CW (a), TW (b), and C4T6W (c) catalysts.

binding energies varied towards the lower region, indicating that an intense interaction existed between Ce and Ti. It was noteworthy that the binding peaks of $Ti^{4+}$ did not appear in the Ti 2p lines. Hence, titanium existed in a $Ti^{4+}$ oxidation state in the CTW catalyst.

To gain a better understanding of the redox properties of the catalysts, $H_2$-TPR measurement was carried out. The $H_2$-TPR profiles of C4T6W, CW, and TW are presented in Fig. 11. Considering the extremely weak reducibility of $TiO_2$, the three TPR peaks centred at 560 ℃, 734 ℃, and 880 ℃ appearing in the TW catalyst were ascribed to the multistage reduction process from $W^{6+}$ to W° (Chen et al., 2011). In the cerium-containing samples, the main TPR peaks shifted to a relatively lower temperature, which suggested that the introduction of Ce contributed to the low-temperature SCR activity. The reduction profile of pure $CeO_2$ consists of two peaks: the low-temperature peak at approximately 497 ℃ and the high-temperature peak at approximately 827 ℃, which is ascribed to the reduction in the surface $CeO_2$ and bulk $CeO_2$, respectively (Liu et al., 2014). For CW and C4T6W, the first peak at around 460 ℃ was assigned to the reduction in surface oxygen, while the peak centred at 620 ℃ was associated with the reduction of the bulk oxygen in ceria (Gao et al., 2010b; Ma et al., 2012). It was notable that CW and C4T6W showed a lower reduction temperature than that of the pure $CeO_2$. The result indicated that an intense interaction existed between Ce and the other metal species. Furthermore, the $H_2$ peak area of each cerium-containing sample could be seen as larger than that of the TW catalyst at low temperature. The results also

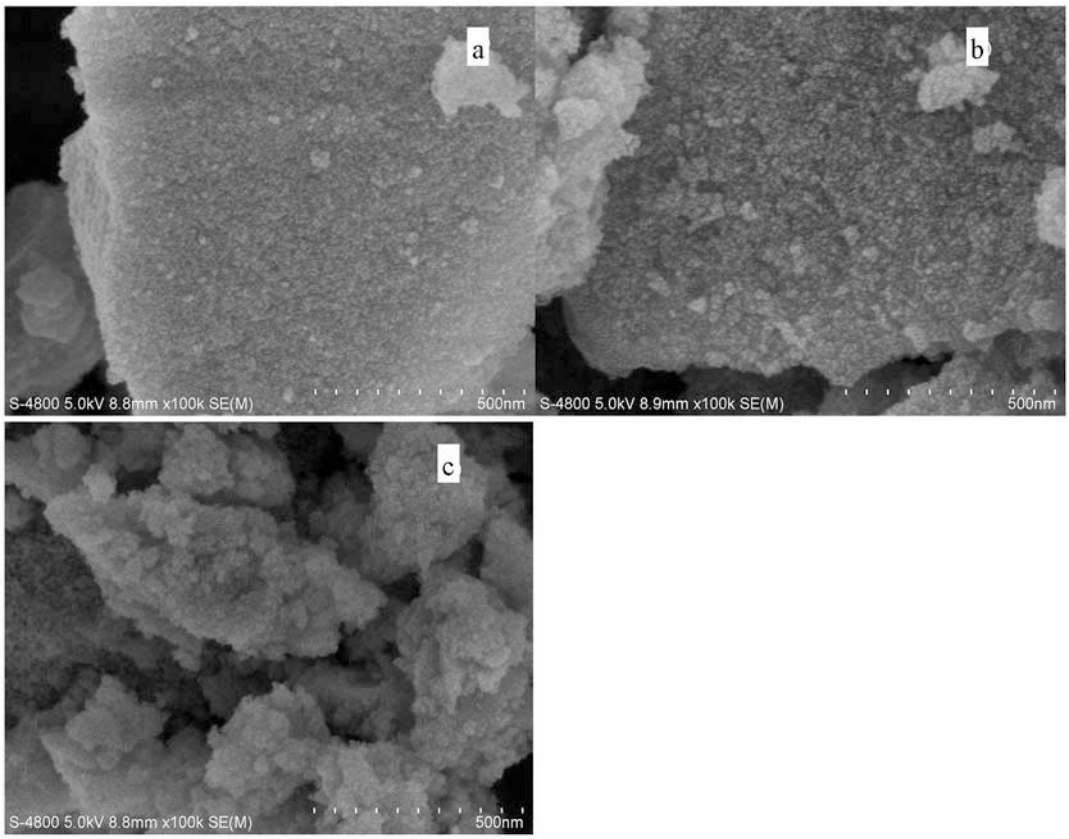


**Fig. 12.** Scanning electron microscopy images for C4T6W (a), TW (b), and CW (c) catalysts.

suggested that the reducibility of the catalysts was enhanced by $CeO_2$ addition, leading directly to the improvement in the low-temperature SCR performance. This conclusion was also consistent with the activity test and XPS analysis.

The morphologies of the C4T6W, TW, and CW catalysts were investigated by SEM images. Similar cakes were observed in the C4T6W and TW particles and these cakes were compact and sharp, being related to the large BET surface area, while the CW particles were the cloud-shaped. The images show the size of the CW particles to be relatively large, signifying that the CW catalyst had a low specific surface area. This result was also in agreement with the result of the BET analysis.

## Conclusions

In this study, the Ce-Ti-W-$O_x$ catalysts obtained by different preparation methods were tested in the $NH_3$-SCR reaction. In addition, the optimal value of the molar ratio of the precursor was obtained. The C4T6W catalyst obtained via the hydrothermal method possessed the highest SCR activity (NO conversion attained more than 90 %) in a broad temperature window of 180–490 ℃ at the GHSV of 60000 $h^{-1}$. In addition, the C4T6W catalyst exhibited high effectivity for NO reduction in a wide range of GHSV from 40000 $h^{-1}$ to 140000 $h^{-1}$. In the stability test, the C4T6W catalyst exhibited a good resistance to $H_2O$ and $SO_2$. The BET and XRD results showed the structure of the C4T6W catalyst to be amorphous; otherwise, the crystallisation of $CeO_2$ which was observed in the cerium-rich samples decreased the BET surface area and negatively affected the SCR performance. It may be concluded from the XPS analysis that a strong interaction exists between Ce, Ti, and W. The Ce-Ti-W-$O_x$ catalysts exhibited a better performance than Ce-W-$O_x$ and Ti-W-$O_x$; this was ascribed to the greater values of the $Ce^{3+}/(Ce^{3+} + Ce^{4+})$ and $O_\alpha/(O_\alpha + O_\beta + O_\gamma)$ ratios. The $H_2$-TPR results also implied that the low-temperature SCR activity was enhanced by the introduction of Ce. As stated above, the Ce-Ti-W-$O_x$ catalysts could be promising candidates for NO abatement from diesel exhausts.

*Acknowledgements. This work was financially supported by the Overseas High-level Talents for Scientific Research (no. 2012ZB002) and the National Natural Science Foundation of China (nos. 21307047 and U1137603).*

## References

Amiridis, M. D., Wachs, I. E., Deo, G., Jehng, J. M., & Kim, D. S. (1996). Reactivity of $V_2O_5$ catalysts for the selective catalytic reduction of NO by $NH_3$: Influence of vanadia loading, $H_2O$, and $SO_2$. *Journal of Catalysis*, *161*, 247–253. DOI: 10.1006/jcat.1996.0182.

Busca, G., Lietti, L., Ramis, G., & Berti, F. (1998). Chemical and mechanistic aspects of the selective catalytic reduction of $NO_x$ by ammonia over oxide catalysts: A review. *Applied Catalysis B: Environmental*, *18*, 1–36. DOI: 10.1016/s0926-3373(98)00040-x.

Chen, L., Li, J. H., Ge, M. F., & Zhu, R. H. (2010). Enhanced activity of tungsten modified $CeO_2/TiO_2$ for selective catalytic reduction of $NO_x$ with ammonia. *Catalysis Today*, *153*, 77–83. DOI: 10.1016/j.cattod.2010.01.062.

Chen, L., Li, J. H., Ablikim, W., Wang, J., Chang, H. Z., Ma, L., Xu, J. Y., Ge, M. F., & Arandiyan, H. (2011). $CeO_2$–$WO_3$ mixed oxides for the selective catalytic reduction of $NO_x$ by $NH_3$ over a wide temperature range. *Catalysis Letters*, *141*, 1859–1864. DOI: 10.1007/s10562-011-0701-4.

Chmielarz, L., Kowalczyk, A., Wojciechowska, M., Boroń, P., Dudek, B., & Michalik, M. (2014). Montmorillonite intercalated with $SiO_2$, $SiO_2$–$Al_2O_3$ or $SiO_2$–$TiO_2$ pillars by surfactant-directed method as catalytic supports for DeNOx process. *Chemical Papers*, *68*, 1219–1227. DOI: 10.2478/s11696-013-0463-0.

Djerad, S., Crocoll, M., Kureti, S., Tifouti, L., & Weisweiler, W. (2006). Effect of oxygen concentration on the $NO_x$ reduction with ammonia over $V_2O_5$–$WO_3/TiO_2$ catalyst. *Catalysis Today*, *113*, 208–214. DOI: 10.1016/j.cattod.2005.11.067.

Ferreira, A. P., Zanchet, D., Rinaldi, R., Schuchardt, U., Damyanova, S., & Bueno, J. M. C. (2010). Effect of the $CeO_2$ content on the surface and structural properties of $CeO_2$–$Al_2O_3$ mixed oxides prepared by sol–gel method. *Applied Catalysis A: General*, *388*, 45–56. DOI: 10.1016/j.apcata.2010.08.033.

Forzatti, P. (2001). Present status and perspectives in de-$NO_x$ SCR catalysis. *Applied Catalysis A: General*, *222*, 221–236. DOI: 10.1016/s0926-860x(01)00832-8.

Gao, X., Jiang, Y., Zhong, Y., Luo, Z. Y., & Cen, K. F. (2010a). The activity and characterization of $CeO_2$–$TiO_2$ catalysts prepared by the sol–gel method for selective catalytic reduction of NO with $NH_3$. *Journal of Hazardous Materials*, *174*, 734–739. DOI: 10.1016/j.jhazmat.2009.09.112.

Gao, X., Jiang, Y., Fu, Y. C., Zhong, Y., Luo, Z. Y., & Cen, K. F. (2010b). Preparation and characterization of $CeO_2/TiO_2$ catalysts for selective catalytic reduction of NO with $NH_3$. *Catalysis Communications*, *11*, 465–469. DOI: 10.1016/j.catcom.2009.11.024.

Gupta, A., Hegde, M. S., Priolkar, K. R., Waghmare, U. V., Sarode, P. R., & Emura, S. (2009). Structural investigation of activated lattice oxygen in $Ce_{1-x}Sn_xO_2$ and $Ce_{1-x-y}Sn_xPd_yO_{2-\delta}$ by EXAFS and DFT calculation. *Chemistry of Materials*, *21*, 5836–5847. DOI: 10.1021/cm902466p.

Jing, L. Q., Xu, Z. L., Sun, X. J., Shang, J., & Cai, W. M. (2001). The surface properties and photocatalytic activities of ZnO ultrafine particles. *Applied Surface Science*, *180*, 308–314. DOI: 10.1016/s0169-4332(01)00365-8.

Lee, K. J., Maqbool, M. S., Kumar, P. A., Song, K. H., & Ha, H. P. (2013). Production from ilmenite of $TiO_2$-supported catalysts for selective catalytic reduction of NO with $NH_3$. *Research on Chemical Intermediates*, *39*, 3265–3277. DOI: 10.1007/s11164-012-0838-9.

Li, L. D., Xue, B., Chen, J. X., Guan, N. J., Zhang, F. X., Liu, D. X., & Feng, H. Q. (2005). Direct synthesis of zeolite coatings on cordierite supports by in situ hydrothermal method. *Applied Catalysis A: General*, *292*, 312–321. DOI: 10.1016/j.apcata.2005.06.015.

Li, J., Han, Y. X., Zhu, Y. H., & Zhou, R. X. (2011). Purification of hydrogen from carbon monoxide for fuel cell application over modified mesoporous CuO–$CeO_2$ catalysts. *Applied Catalysis B: Environmental*, *108–109*, 72–80. DOI: 10.1016/j.apcatb.2011.08.010.

Li, X. L., Li, Y. H., Deng, S. S., & Rong, T. A. (2013). A Ce–Sn–$O_x$ catalyst for the selective catalytic reduction of

$NO_x$ with $NH_3$. *Catalysis Communications*, *40*, 47–50. DOI: 10.1016/j.catcom.2013.05.024.

Liu, H. D., Wei, L. Q., Yue, R. L., & Chen, Y. F. (2010). $CrO_x$-$CeO_2$ binary oxide as a superior catalyst for NO reduction with $NH_3$ at low temperature in presence of CO. *Catalysis Communications*, *11*, 829–833. DOI: 10.1016/j.catcom.2010.03.002.

Liu, F. D., Asakura, K., He, H., Shan, W. P., Shi, X. Y., & Zhang, C. B. (2011). Influence of sulfation on iron titanate catalyst for the selective catalytic reduction of $NO_x$ with $NH_3$. *Applied Catalysis B: Environmental*, *103*, 369–377. DOI: 10.1016/j.apcatb.2011.01.044.

Liu, C. X., Chen, L., Chang, H. Z., Ma, L., Peng, Y., Arandiyan, H., & Li, J. H. (2013). Characterization of $CeO_2$–$WO_3$ catalysts prepared by different methods for selective catalytic reduction of $NO_x$ with $NH_3$. *Catalysis Communications*, *40*, 145–148. DOI: 10.1016/j.catcom.2013.06.017.

Liu, Z. M., Zhang, S. X., Li, J. H., & Ma, L. L. (2014). Promoting effect of $MoO_3$ on the $NO_x$ reduction by $NH_3$ over $CeO_2/TiO_2$ catalyst studied with in situ DRIFTS. *Applied Catalysis B: Environmental*, *144*, 90–95. DOI: 10.1016/j.apcatb.2013.06.036.

Long, R. Q., & Yang, R. T. (1999). Selective catalytic reduction of nitrogen oxides by ammonia over $Fe^{3+}$-exchanged $TiO_2$-pillared clay catalysts. *Journal of Catalysis*, *186*, 254–268. DOI: 10.1006/jcat.1999.2558.

Ma, Z. R., Weng, D., Wu, X. D., Si, Z. C., & Wang, B. (2012). A novel Nb–Ce/$WO_x$–$TiO_2$ catalyst with high $NH_3$-SCR activity and stability. *Catalysis Communications*, *27*, 97–100. DOI: 10.1016/j.catcom.2012.07.006.

Ma, L. N., Qu, H. X., Zhang, J., Tang, Q. S., Zhang, S. L., & Zhong, Q. (2013). Preparation of nanosheet Fe-ZSM-5 catalysts, and effect of Fe content on acidity, water, and sulfur resistance in the selective catalytic reduction of $NO_x$ by ammonia. *Research on Chemical Intermediates*, *39*, 4109–4120. DOI: 10.1007/s11164-012-0927-9.

Martínez-Franco, R., Moliner, M., Franch, C., Kustov, A., & Corma, A. (2012). Rational direct synthesis methodology of very active and hydrothermally stable Cu-SAPO-34 molecular sieves for the SCR of $NO_x$. *Applied Catalysis B: Environmental*, *127*, 273–280. DOI: 10.1016/j.apcatb.2012.08.034.

Pantazis, C. C., Trikalitis, P. N., & Pomonis, P. J. (2005). Highly loaded and thermally stable Cu-containing mesoporous silica – Active catalyst for the NO + CO reaction. *The Journal of Physical Chemistry B*, *109*, 12574–12581. DOI: 10.1021/jp0516689.

Peng, Y., Li, K. Z., & Li, J. H. (2013). Identification of the active sites on $CeO_2$–$WO_3$ catalysts for SCR of $NO_x$ with $NH_3$: An *in situ* IR and Raman spectroscopy study. *Applied Catalysis B: Environmental*, *140–141*, 483–492. DOI: 10.1016/j.apcatb.2013.04.043.

Qu, R. Y., Gao, X., Cen, K. F., & Li, J. H. (2013). Relationship between structure and performance of a novel cerium-niobium binary oxide catalyst for selective catalytic reduction of NO with $NH_3$. *Applied Catalysis B: Environmental*, *142*, 290–297. DOI: 10.1016/j.apcatb.2013.05.035.

Reddy Inturi, S. N., Boningari, T., Suidan, M., & Smirniotis, P. G. (2014). Visible-light-induced photodegradation of gas phase acetonitrile using aerosol-made transition metal (V, Cr, Fe, Co, Mn, Mo, Ni, Cu, Y, Ce, and Zr) doped $TiO_2$. *Applied Catalysis B: Environmental*, *144*, 333–342. DOI: 10.1016/j.apcatb.2013.07.032.

Ruggeri, M. P., Grossale, A., Nova, I., Tronconi, E., Jirglova, H., & Sobalik, Z. (2012). FTIR in situ mechanistic study of the $NH_3$—$NO/NO_2$ "Fast SCR" reaction over a commercial Fe-ZSM-5 catalyst. *Catalysis Today*, *184*, 107–114. DOI: 10.1016/j.cattod.2011.10.036.

Schneider, H., Scharf, U., Wokaun, A., & Baiker, A. (1994). Chromia on titania: IV. Nature of active sites for selective catalytic reduction of NO by $NH_3$. *Journal of Catalysis*, *146*, 545–556. DOI: 10.1006/jcat.1994.1093.

Shan, W. P., Liu, F. D., He, H., Shi, X. Y., & Zhang, C. B. (2012). A superior Ce-W-Ti mixed oxide catalyst for the selective catalytic reduction of $NO_x$ with $NH_3$. *Applied Catalysis B: Environmental*, *115*, 100–106. DOI: 10.1016/j.apcatb.2011.12.019.

Worch, D., Suprun, W., & Gläser, R. (2014). Fe- and Cu-oxides supported on $\gamma$-$Al_2O_3$ as catalysts for the selective catalytic reduction of NO with ethanol. Part I: catalyst preparation, characterization, and activity. *Chemical Papers*, *68*, 1228–1239. DOI: 10.2478/s11696-013-0533-3.

Wu, Z. B., Jin, R. B., Wang, H. Q., & Liu, Y. (2009). Effect of ceria doping on $SO_2$ resistance of $Mn/TiO_2$ for selective catalytic reduction of NO with $NH_3$ at low temperature. *Catalysis Communications*, *10*, 935–939. DOI: 10.1016/j.catcom.2008.12.032.

Yang, S. J., Wang, C. Z., Li, J. H., Yan, N. Q., Ma, L., & Chang, H. Z. (2011). Low temperature selective catalytic reduction of NO with $NH_3$ over Mn–Fe spinel: Performance, mechanism and kinetic study. *Applied Catalysis B: Environmental*, *110*, 71–80. DOI: 10.1016/j.apcatb.2011.08.027.

Zamaro, J. M., & Miró, E. E. (2010). Novel binderless zeolite-coated monolith reactor for environmental applications. *Chemical Engineering Journal*, *165*, 701–708. DOI: 10.1016/j.cej.2010.10.014.

Zhang, S. L., Li, H. Y., & Zhong, Q. (2012). Promotional effect of F-doped $V_2O_5$–$WO_3/TiO_2$ catalyst for $NH_3$-SCR of NO at low-temperature. *Applied Catalysis A: General*, *435–436*, 156–162. DOI: 10.1016/j.apcata.2012.05.049.